Supporting information for:

NO_2 suppression of autoxidation - inhibition of gas-phase highly-oxidized dimer product formation

Matti P. Rissanen*

Institute for Atmospheric and Earth System Research (INAR), University of Helsinki, Finland.

Email: matti.p.rissanen@helsinki.fi

Methods

Cyclohexene (c-C_6H_{10}) oxidation was investigated in 2.4 and 7.6 cm inner diameter and 100 to 200 cm length flow tubes under ambient atmospheric conditions (T = 293 ± 3 K, p = 1 Atm). Gas flow rate inside the flow tube was determined by the sampling need of the chemical ionization inlet, which was at around 10 liters per minute (lpm) and resulted in laminar flow conditions and residence times between 2 and 20 seconds. The carrier gases used were nitrogen (Aga, N_2, purity 5.0) and synthetic air (Aga, N_2 and O_2, purity 5.0). Nitrogen dioxide and nitrogen oxide used were 50 parts per million (ppm) mixtures with N_2 as the pressure gas (Aga, NO/NO_2, 50 ppm in N_2). Ozone was produced by a commercial ozone generator (UVP products SOG-3) from the synthetic air (or filtered and pressurized air) and its concentration was monitored by an ozone analyzer (Thermo Scientific model 49). Cyclohexene was obtained from Sigma-Aldrich (≥99% purity), and its concentration in the experiment was determined by the pure compound vapor pressure and dilution factors in the gas flow system. Detection of the oxidized intermediates and products was accomplished by means of chemical ionization mass spectrometry (CIMS) applying nitrate (NO_3^-) reagent ions to cluster with the target compounds. This technique was originally devised to selectively detect atmospheric sulfuric acid and has recently been devoted for studying highly-oxidized multifunctional organic compounds (HOM) resulting from hydrocarbon autoxidation. The mass spectrometer utilized was an atmospheric pressure interface time-of-flight instrument manufactured by TofWerk (APi-ToF, Tofwerk Ltd, Thun, Switzerland). Schematic of the experimental setup is given in Figure S1.

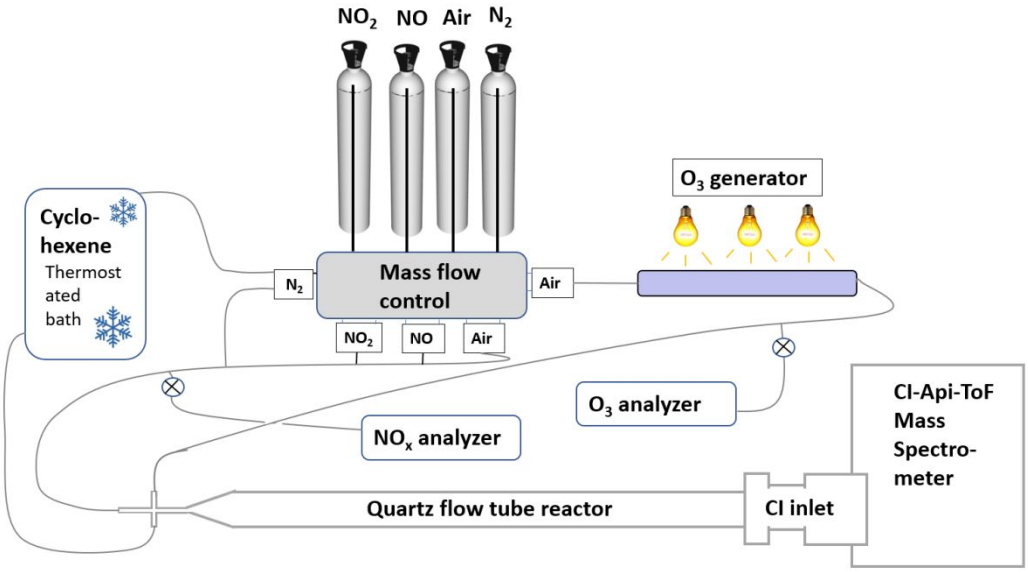

Figure S1 Schematic of the experimental setup.

The experiments were conducted under various concentrations of cyclohexene ([*c*-C_6H_{10}] = (3-235) × 10^{13} cm^{-3} [=3 to 96 ppm]), ozone ([O_3] = (1.23-14.8) × 10^{11} cm^{-3} [=5 to 60 ppb]), NO_x ([NO_2] = (1.27-63.4) × 10^{12} cm^{-3} [=51 to 2577 ppb]; [NO] = (1.27-10.1) × 10^{12} cm^{-3} [=51 to 412 ppb]), and reaction time (t = 2.2-22.4 s), constituting a wide range of experimental conditions with different oxidative capacity and potential for product formation.

Charging probabilities and transmission, and their influence on measured concentrations

NO_3^- ionization has been frequently applied in quantifying HOM product signals, with a calibration procedure utilizing SO_2 + OH (+H_2O) derived H_2SO_4 to determine the lower limit concentrations of the products observed. This analysis relies on the assumption that HOM products experience the same collision limit charging in the chemical ionization inlet as does sulfuric acid. In addition, Ehn et al.[1] have further rationalized the measured concentrations by using further empirical constraints and arrived into good agreement with the single-calibration-factor procedure. On the other hand, the detection efficiency of NO_3^- charging is known to depend on the available H-bond donating functional groups and on the number of O-atoms in the structure, both increasing the detection sensitivity and thus leading to a positive bias relative to the less oxidized compounds[2, 3]. The sensitivity is further

dependent on the detailed settings of the atmospheric pressure interface (APi) altering the ion transmission in the mass range of interest[4]. In considering these issues it becomes clear how difficult it is to adequately account for the compound specific detection sensitivity, and thus this was not attempted here, and instead all the concentrations are given as measured ion signals in ion counts per second (cps), and where relevant (i.e., to be able to compare signals), they are normalized to the total reagent ion current which was c.a. 10 000 to 20 000 cps.

Oxidation pathways

The product peaks detected in cyclohexene ozonolysis experiments without addition of NO_x have been collected to Table S1.

Table S1 The most prominent mass peaks measured without NO_x addition to the gas mixture.

Without NO_x							
[a, c] $C_4H_6O_4$	[c] $C_5H_8O_4$	[c] $C_6H_{10}O_4$	$C_4H_6O_4$	$C_6H_{10}O_3$	$C_5H_8O_4$	$C_6H_{10}O_4$	$C_5H_8O_5$
[b] 117.0193	131.0350	145.0506	180.0150	192.0514	194.0306	208.0463	210.0250
$C_5H_{10}O_5$	$C_6H_8O_5$	$C_6H_{10}O_5$	$C_5H_9O_6$	$C_5H_{10}O_6$	$C_6H_8O_6$	$C_6H_9O_6$	$C_6H_{10}O_6$
212.0412	222.0255	224.0412	227.0283	228.0283	238.0205	239.0283	240.0361
$C_6H_{11}O_6$	$C_6H_8O_7$	$C_6H_9O_7$	$C_6H_{10}O_7$	$C_6H_{11}O_7$	$C_6H_8O_8$	$C_6H_8O_9$	$C_6H_{10}O_8$
241.0439	254.0154	255.0232	256.0310	257.0388	270.0103	271.0181	272.0259
$C_6H_8O_9$	$C_6H_9O_9$	$C_6H_{10}O_9$	$C_6H_7O_{10}$	$C_6H_7O_{10}$	$C_6H_8O_{10}$	$C_6H_9O_{10}$	$C_6H_9O_{10}$
286.0052	287.0052	288.0052	300.9923	300.9923	302.0001	303.0079	303.0079
$C_6H_{10}O_{10}$	$C_6H_{11}O_{10}$	$C_{11}H_{18}O_7$	$C_{11}H_{20}O_7$	$C_{12}H_{20}O_7$	$C_{12}H_{18}O_8$	$C_{11}H_{18}O_9$	$C_{11}H_{20}O_9$
304.0158	305.0236	324.0936	326.1093	338.1093	352.0885	356.0834	358.0991
$C_{12}H_{18}O_9$	$C_{12}H_{20}O_9$	$C_{11}H_{18}O_{10}$	$C_{12}H_{16}O_{10}$	$C_{12}H_{18}O_{10}$	$C_{12}H_{20}O_{10}$	$C_{11}H_{18}O_{11}$	$C_{12}H_{18}O_{11}$
368.0834	370.0991	372.0784	382.0784	384.0784	386.0940	388.0733	400.0733
$C_{11}H_{18}O_{12}$	$C_{12}H_{18}O_{12}$	$C_{12}H_{16}O_{13}$	$C_{12}H_{18}O_{13}$	$C_{11}H_{16}O_{14}$	$C_{12}H_{16}O_{14}$	$C_{12}H_{18}O_{14}$	$C_{12}H_{18}O_{15}$
404.0682	416.0676	430.0475	432.0631	434.0424	446.0424	448.0580	464.0529

[a] Observed product composition, and [b] its exact mass in the spectrum (including the mass of NO_3^- of 61.9884 Th). [c] Detected as deprotonated product ion; does not include NO_3^- mass. All masses are given in Thomson units; 1 Th = u/e, where e is elementary charge and u is the atomic mass unit.

Due to cyclohexenes symmetric ring structure with no substituents around the double bond, it produces two aldehyde functionalities containing primary oxidation products as illustrated in Figure 1. In these compounds the aldehydic hydrogens have the lowest C-H bond energies, and thus further oxidation, autoxidation or stepwise, will inevitably lead into further acylperoxy radicals. Also, cyclohexene's carbon chain length enables close to optimal H-shift transition states[6] and facilitate the formation of a pool of secondary acylperoxy radicals. In Scheme S1 further examples for acylperoxy radical formation during the oxidation sequence have been gathered.

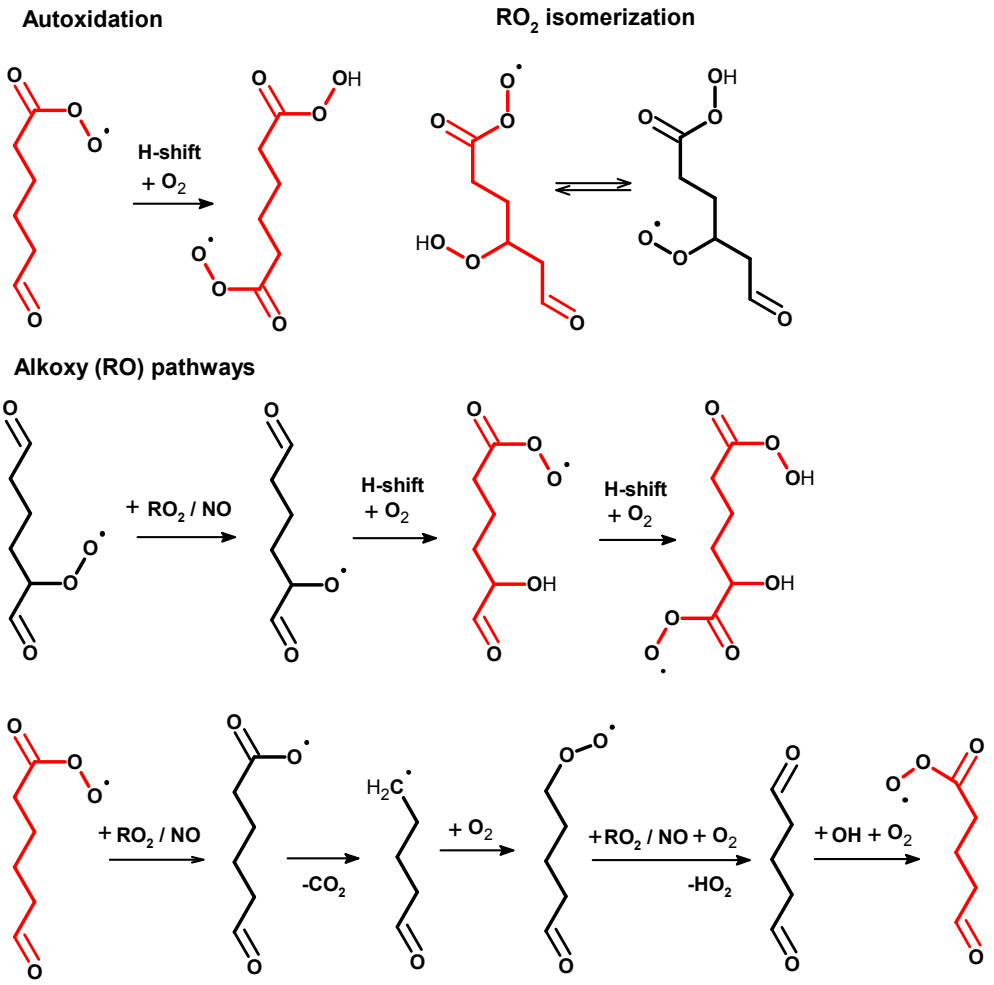

Scheme S1 Further potential acylperoxy formation pathways, and interconversions, during cyclohexene autoxidation**.** Acylperoxy radicals have been marked with red color.

The pool of different $RC(O)O_2$ will combine with NO_2 forming a collection of peroxyacylnitrate (PAN) species ($R(C)O_2NO_2$). Potential PAN structures detected in the current work have been collected in Figure S2.

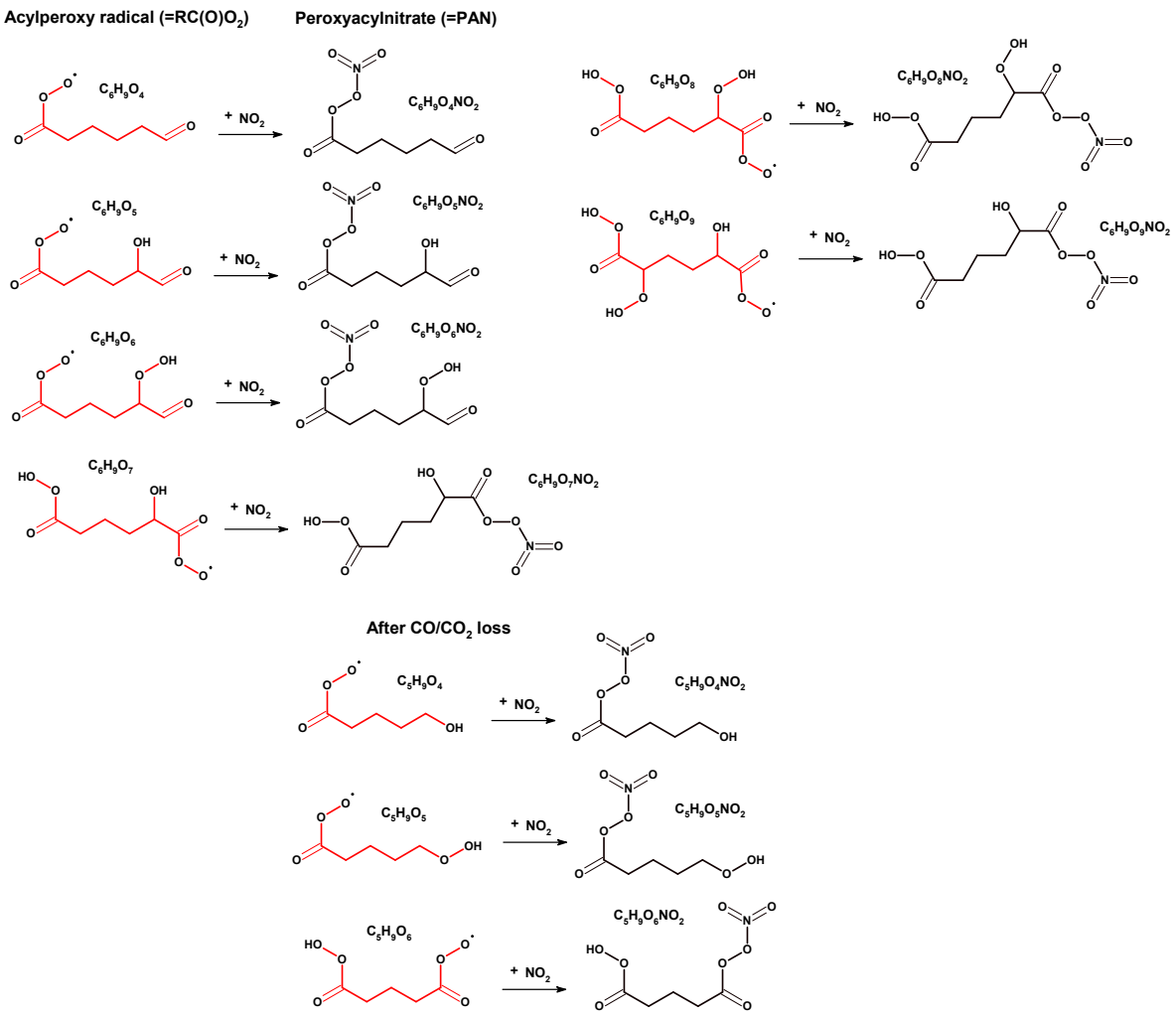

Figure S2 Potential peroxyacylnitrate (PAN) product structures detected in this work. Acylperoxy radicals have been marked with red color.

Suppression reaction kinetics

The suppressing reaction $RC(O)O_2 + NO_2$ must happen faster than the unimolecular hydrogen shifts progressing the oxidation chain reaction. Previously it has been estimated that H-shift rates of above 0.1 s^{-1} can compete with other RO_2 loss processes (mainly reactions with HO_2 and NO) even under moderately polluted atmospheres[6]. The exact concentration at which NO_2 will suppress depends on the rate of the $RO_2 + NO_2$ reaction, and thus on the specific RO_2. The experimental rate determinations for $RO_2 + NO_2$ are scarce, especially for the larger RO_2 as relevant for the current investigation, and hence, the exact values cannot be used. However, the limiting

concentrations at which the NO_2 reaction becomes competitive with the unimolecular propagation reaction can be estimated using hypothetical rate coefficient values. In Table S2 the concentration of NO_2 that is needed for the $RC(O)O_2 + NO_2$ reaction to outcompete an H-shift rate of 0.1 s^{-1} and 10 s^{-1} have been calculated assuming general and previously determined rate coefficient values. In Figure 3, a similar analysis was illustrated in graphical format with general assumed reaction rate $k(RC(O)O_2+NO_2)$ between 10^{-10} cm^3s^{-1} and 10^{-13} cm^3s^{-1} depicted as a function of $[NO_2]$.

Table S2 NO_2 concentration needed to outcompete H-shift rates of 0.1 s^{-1} and 10 s^{-1}; competition of unimolecular H-shift and bimolecular $RC(O)O_2 + NO_2$ reaction rates.

$[NO_2]$ / cm^{-3} (ppb)	**$k(RC(O)O_2+NO_2)$ / cm^3 s^{-1}**	**$k'(RC(O)O_2+NO_2)$ / s^{-1}**	**Comment**
10^{12} (40.7)	1 x 10^{-13}	0.1	Slowish *k* value
10^{14} (4065)	1 x 10^{-13}	10	
10^{11} (4.1)	1 x 10^{-12}	0.1	
10^{13} (406.5)	1 x 10^{-12}	10	
1.14 × 10^{10} (0.46)	8.8 x 10^{-12}	0.1	$k(C_2H_5O_2+NO_2)$ used
1.14 × 10^{12} (46.2)	8.8 x 10^{-12}	10	
6.67 × 10^9 (0.27)	1.5 x 10^{-11}	0.1	$k(CH_3C(O)O_2+NO_2)$ used
6.67 × 10^{11} (27.1)	1.5 x 10^{-11}	10	
1.11 × 10^9 (0.05)	9 x 10^{-11}	0.1	*k* close to collision limit
1.11 × 10^{11} (4.51)	9 x 10^{-11}	10	

According to the simple comparison procedure above it was estimated with previously measured $RC(O)O_2 + NO_2$ and $RO_2 + NO_2$ rate coefficients that already below 1 ppb of NO_2, corresponding to very clean environmental conditions, can influence the oxidation sequence. With a moderate rate coefficient of $k(RC(O)O_2+NO_2) = 5 \times 10^{-12}$ cm^3 $molecule^{-1}$ s^{-1}, over 50% of the acylperoxy radicals would be lost to PAN formation if the potential secondary chemistry is omitted. At a hundred-fold higher NO_2 concentration, corresponding to polluted urban environments around the world, most of the $RC(O)O_2$ would be more likely to form PAN than HOM, in this simple analysis.

NO's enhancing influence

In contrast to $RO_2 + NO_2$ reaction, $RO_2 + NO$ reaction can also propagate the radical chain by reactive RO generation. In experiments where the NO's influence was investigated, an enhanced $C_6H_8O_8$ product formation was observed after NO was introduced into the gas flow, whereas larger oxidation products were strongly depleted (Figure S3). The amplification of RO chemistry due to NO could lead to species with C5 and C11 structures, i.e., to compounds which have lost a CO or CO_2 during the oxidation sequence. Whereas a C5 compound was observed to increase with the NO addition (see Figure S3), all the dimer compounds were depleted as a function of $[NO_x]$, and thus this dependence could not be observed for C11 compounds. Due to the cyclic nature of the oxidation chain reaction, yet further NO addition interfered the oxidation at an even earlier stage, and resulted also in reduction of the observed nitrate formation (Figure S4).

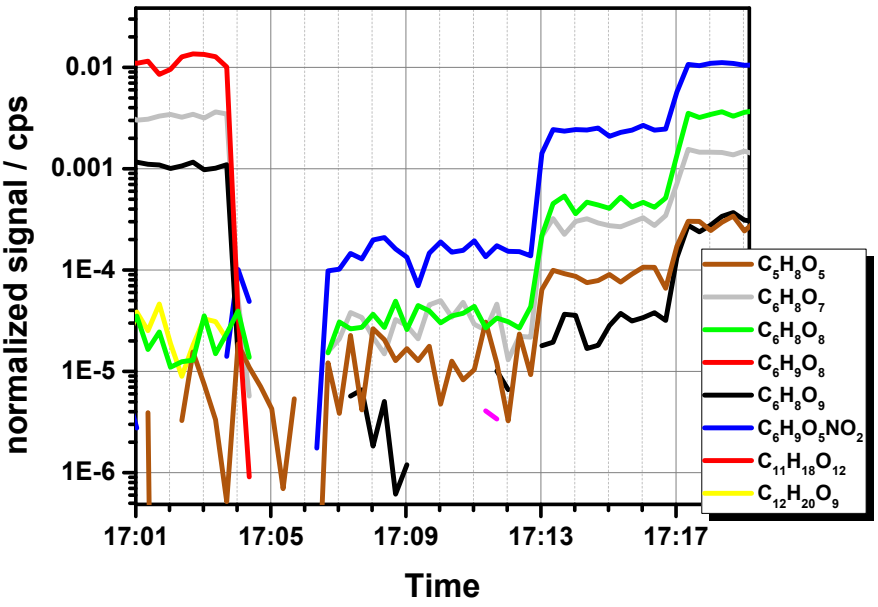

Figure S3 $C_6H_8O_8$ product formation is aided by NO addition. Note also that $C_6H_8O_7$ is produced in bigger proportion, whereas the $C_6H_9O_8$ radical and $C_6H_8O_9$ closed shell product are strongly depleted.

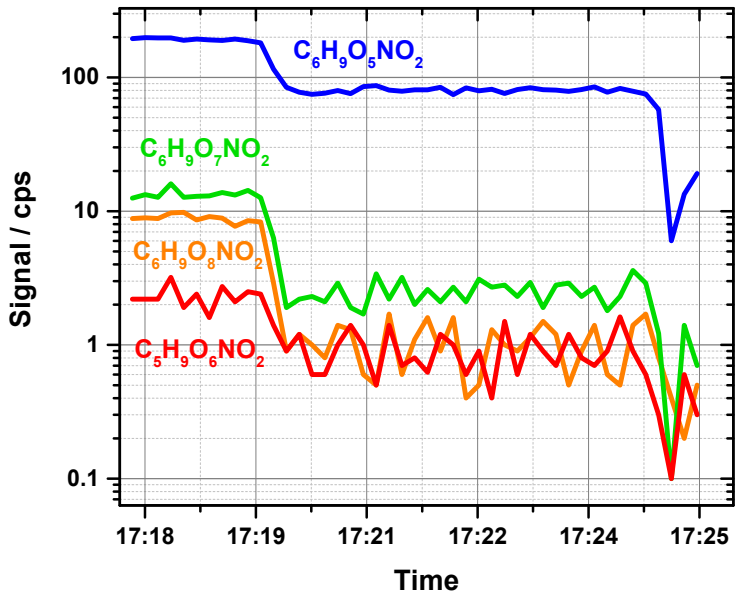

Figure S4 even the observed nitrate signals were plummeting at highest NO or NO_2 additions.

The addition of NO_x during various instances of the oxidation sequence is illustrated in Figure S5, where example spectra obtained at several [NO_2] and [RO_2] combinations are shown.

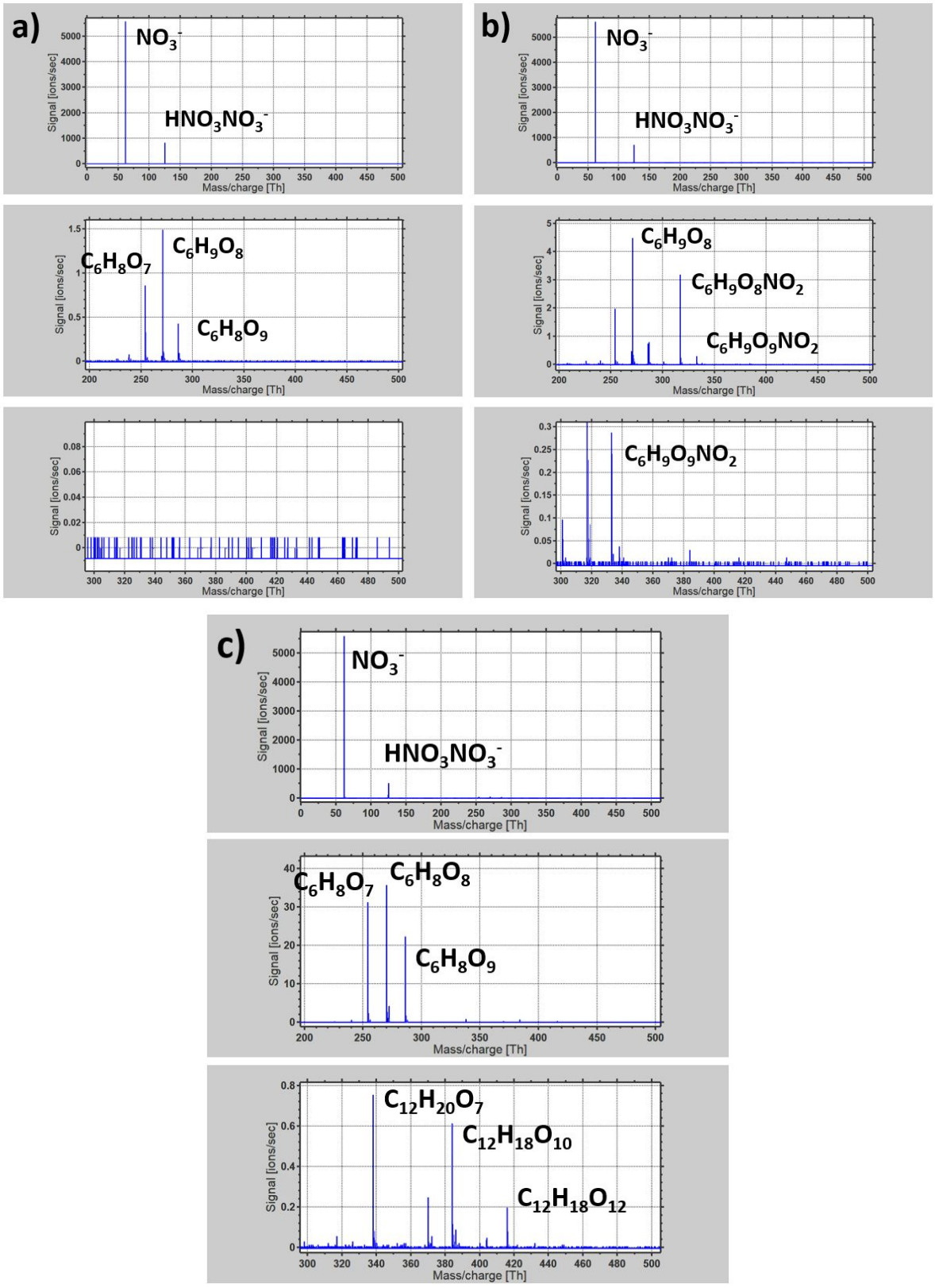
a)
NO_3^-
$HNO_3NO_3^-$
$C_6H_8O_7$
$C_6H_9O_8$
$C_6H_8O_9$
b)
NO_3^-
$HNO_3NO_3^-$
$C_6H_9O_8$
$C_6H_9O_8NO_2$
$C_6H_9O_9NO_2$
$C_6H_9O_9NO_2$
c)
NO_3^-
$HNO_3NO_3^-$
$C_6H_8O_7$
$C_6H_8O_8$
$C_6H_8O_9$
$C_{12}H_{20}O_7$
$C_{12}H_{18}O_{10}$
$C_{12}H_{18}O_{12}$
Signal [ions/sec]
Mass/charge [Th]

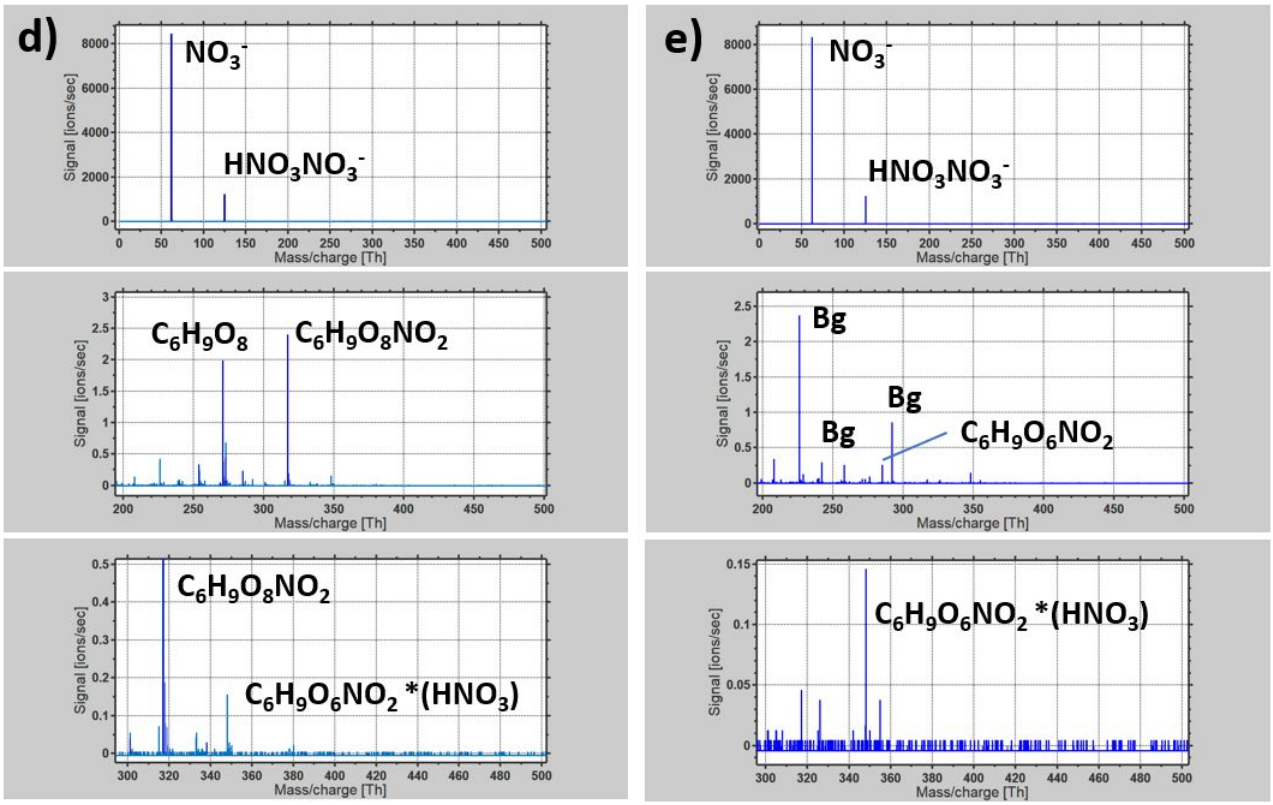

Figure S5 Panels **a)** to **e)** illustrate how NO_x addition happens during various times of the oxidation sequence. The experiments were performed in 2.4 cm i.d. and either 80 or 200 cm long Quartz reactor, with $[O_3]$ = 11 ppb and $[O_2]$ = 4.5 %. The spectra were obtained at: **a)** $[NO_2]$ = 0 and low $[RO_2]$ ($[CH] = 3 \times 10^{13}$ cm^{-3}) at 2.2 s reaction time; **b)** $[NO_2]$ = 50 ppb, and moderate $[RO_2]$ ($[CH] = 1.3 \times 10^{14}$ cm^{-3}) at 5.9 second reaction time; **c)** $[NO_2]$ = 0 and high $[RO_2]$ ($[CH] = 6.6 \times 10^{14}$ cm^{-3}) at 5.9 second reaction time; **d)** $[NO_2]$ = 500 ppb and high $[RO_2]$ ($[CH] = 6.6 \times 10^{14}$ cm^{-3}) at 5.9 second reaction time; and **e)** $[NO_2]$ = 2600 ppb and high $[RO_2]$ ($[CH] = 6.6 \times 10^{14}$ cm^{-3}) at 5.9 second reaction time. Bg stands for a background peak.

With the highest NO_x additions, the oxidation suppression was observed even earlier in the oxidation chain, which resulted in decrease of all the product species detected with the utilized nitrate ionization technique (See Figures S4 and S5 above). In the experiments with very high RO_2 and NO_x concentrations, it was impossible to even qualitatively quantify the extent of NO_2 suppression, as removing NO_2 from the gas flow resulted in strong

depletion of the reagent ion signals (indicating formation of a very large number of products), and thus rendered the CIMS concentration determination unreliable. However, when a sufficient NO_2 flow was added back to the reacting gas mixture, the HOM formation (except few PAN-HOM) practically ceased, and the reagent ion signals recovered (see Figure 2).

Also, in experiments with high [RO_2] and [NO_x], apparent highly oxidized nitrates with two N-atoms attached were observed and could potentially indicate formation by NO_3 initiated and NO_x terminated reactions [i.e., $C_6H_{10}O_6NO_3NO_2(*NO_3^-)$ at 348.017 Th, see Table 1 and Figure S5]. However, product charged by the reagent ion dimer would be observed with a similar composition {i.e., $m/z[C_6H_9O_6NO_2(*HNO_3NO_3^-)] = m/z[C_6H_{10}O_6NO_3NO_2(*NO_3^-)]$} and seems far more likely, already as the NO_3 is not expected to live long in enough here to perturb the oxidation system. Also, from Figure S5 e it can be seen that when most of the compounds have been depleted due to high [NO_2] in the flow, the two peaks that are well resolvable in the spectrum, and have about similar intensity, could correspond to $C_6H_9O_6NO_2$ charged by NO_3^- and $HNO_3NO_3^-$. Also in other experiments, the apparently two nitrogen containing compounds were coincident with the highest PAN signals and could be explained with these PAN species clustering with the reagent dimer; similar observations of potential dimer charging were absent from experiments conducted without NO_x. Finally, it seems that the nitrate functionality containing products could potentially cluster more efficiently with NO_3^-, and thus potentially also by $HNO_3NO_3^-$, as the PAN signals seem to increase somewhat more than the HOM signals decrease, indicating a potential positive bias in their detection.

References

1. M. Ehn, J. A. Thornton, E. Kleist, M. Sipilä, H. Junninen, I. Pullinen, M. Springer, F. Rubach, R. Tillmann, B. Lee, F. Lopez-Hilfiker, S. Andres, I.-H. Acir, M. Rissanen, T. Jokinen, S. Schobesberger, J. Kangasluoma, J. Kontkanen, T. Nieminen, T. Kurtén, L. B. Nielsen, S. Jørgensen, H. G. Kjaergaard, M. Canagaratna, M. Dal Maso, T. Berndt, T. Petäjä, A. Wahner, V.-M. Kerminen, M. Kulmala, D. R.

Worsnop, J. Wildt, T. F. Mentel, A large source of low-volatility secondary organic aerosol, Nature, 2014, 506, 476-479.

2. N. Hyttinen, O. Kupiainen-Määttä, M. P. Rissanen, M. Muuronen, M. Ehn, T. Kurtén, Modeling the Detection of Highly Oxidized Cyclohexene Ozonolysis Products Using Nitrate-Based Chemical Ionization, J. Phys. Chem. A, 2015, 119, 6339-6345.
3. N. Hyttinen, R. V. Otkjær, S. Iyer, H. G. Kjaergaard, M. P. Rissanen, P. O. Wennberg, T. Kurteń, Computational Comparison of Different Reagent Ions in the Chemical Ionization of Oxidized Multifunctional Compounds, J. Phys. Chem. A, 2018, 122, 269-279.
4. M. Heinritzi, M. Simon, G. Steiner, A. C. Wagner, A. Kürten, A. Hansel, J. Curtius, Characterization of the mass-dependent transmission efficiency of a CIMS, Atmos. Meas. Tech., 2016, 9, 1449-1460.
5. M. P. Rissanen, T. Kurtén, M. Sipilä, J. A. Thornton, J. Kangasluoma, N. Sarnela, H. Junninen, S. Jørgensen, S. Schallhart, M. K. Kajos, R. Taipale, M. Springer, T. F. Mentel, T. Ruuskanen, T. Petäjä, D. R. Worsnop, H. G. Kjaergaard, M. Ehn, The formation of highly oxidized multifunctional products in the ozonolysis of cyclohexene, J. Am. Chem. Soc., 2014, 136, 15596-15606.
6. J. D. Crounse, L. B. Nielsen, S. Jørgensen, H. G. Kjaergaard, P. O. Wennberg, Autoxidation of Organic Compounds in the Atmosphere, J. Phys. Chem. Lett., 2013, 4, 3513-3520.